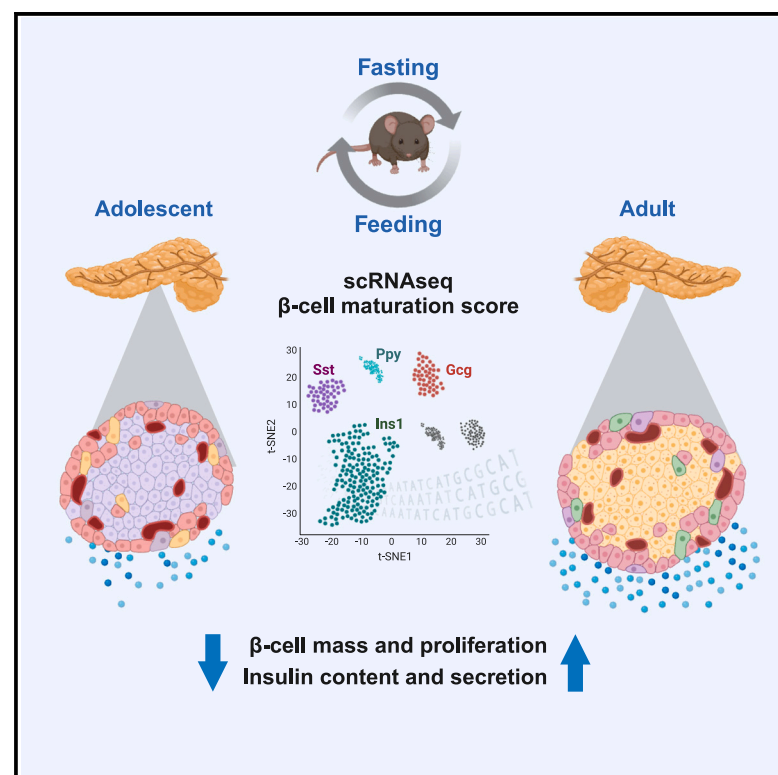


# Chronic intermittent fasting impairs $\beta$ cell maturation and function in adolescent mice

## Graphical abstract



## Authors

Leonardo Matta, Peter Weber, Suheda Erener, ..., Heiko Lickert, Alexander Bartelt, Stephan Herzig

## Correspondence

alexander.bartelt@med.uni-muenchen.de (A.B.),  
stephan.herzig@helmholtz-muenchen.de (S.H.)

## In brief

Intermittent fasting (IF) is generally associated with improved metabolism, but whether there are age-dependent limitations of IF needs to be explored. Matta et al. now demonstrate that while IF improved  $\beta$  cell function in old and middle-aged mice, long-term IF impaired  $\beta$  cell maturation and function in adolescent mice.

## Highlights

- Short-term IF improves glucose homeostasis without altering islet function
- Long-term IF impairs  $\beta$  cell function and maturation in adolescent mice
- Impaired  $\beta$  cell function is associated with lower numbers of mature cells
- Diminished maturation of  $\beta$  cells is linked to human type 1 diabetes



## Report

# Chronic intermittent fasting impairs $\beta$ cell maturation and function in adolescent mice

Leonardo Matta,<sup>1,2,11</sup> Peter Weber,<sup>1,11</sup> Suheda Erener,<sup>1,11</sup> Alina Walth-Hummel,<sup>1,3,4</sup> Daniela Hass,<sup>1</sup> Lea K. Bühler,<sup>1,3,4</sup> Katarina Klepac,<sup>1</sup> Julia Szendroedi,<sup>1,3,4</sup> Joel Guerra,<sup>1,2</sup> Maria Rohm,<sup>1,3,4</sup> Michael Sterr,<sup>4,5</sup> Heiko Lickert,<sup>4,5,6</sup> Alexander Bartelt,<sup>1,2,4,7,8,9,\*</sup> and Stephan Herzig<sup>1,2,3,4,7,10,12,\*</sup>

<sup>1</sup>Institute for Diabetes and Cancer (IDC), Helmholtz Center Munich, German Research Center for Environmental Health, Neuherberg, Germany

<sup>2</sup>Institute for Cardiovascular Prevention (IPEK), Faculty of Medicine, Ludwig-Maximilians-Universität München, Munich, Germany

<sup>3</sup>Joint Heidelberg-IDC Translational Diabetes Program, Inner Medicine 1, Heidelberg University Hospital, Heidelberg 69120, Germany

<sup>4</sup>German Center for Diabetes Research, 85764 Neuherberg, Germany

<sup>5</sup>Institute of Diabetes and Regeneration Research, Helmholtz Munich, Neuherberg, Germany

<sup>6</sup>School of Medicine, Technical University of Munich (TUM), Munich, Germany

<sup>7</sup>German Center for Cardiovascular Research, Partner Site Munich Heart Alliance, Technische Universität München, Munich, Germany

<sup>8</sup>Chair of Translational Nutritional Medicine, TUM School of Life Sciences, Research Department of Molecular Life Sciences, Technical University of Munich, Freising, Germany

<sup>9</sup>Else Kröner Fresenius Center for Nutritional Medicine, Technical University of Munich, Munich, Germany

<sup>10</sup>Chair Molecular Metabolic Control, Technical University Munich, Munich 80333, Germany

<sup>11</sup>These authors contributed equally

<sup>12</sup>Lead contact

\*Correspondence: [alexander.bartelt@med.uni-muenchen.de](mailto:alexander.bartelt@med.uni-muenchen.de) (A.B.), [stephan.herzig@helmholtz-muenchen.de](mailto:stephan.herzig@helmholtz-muenchen.de) (S.H.)

<https://doi.org/10.1016/j.celrep.2024.115225>

## SUMMARY

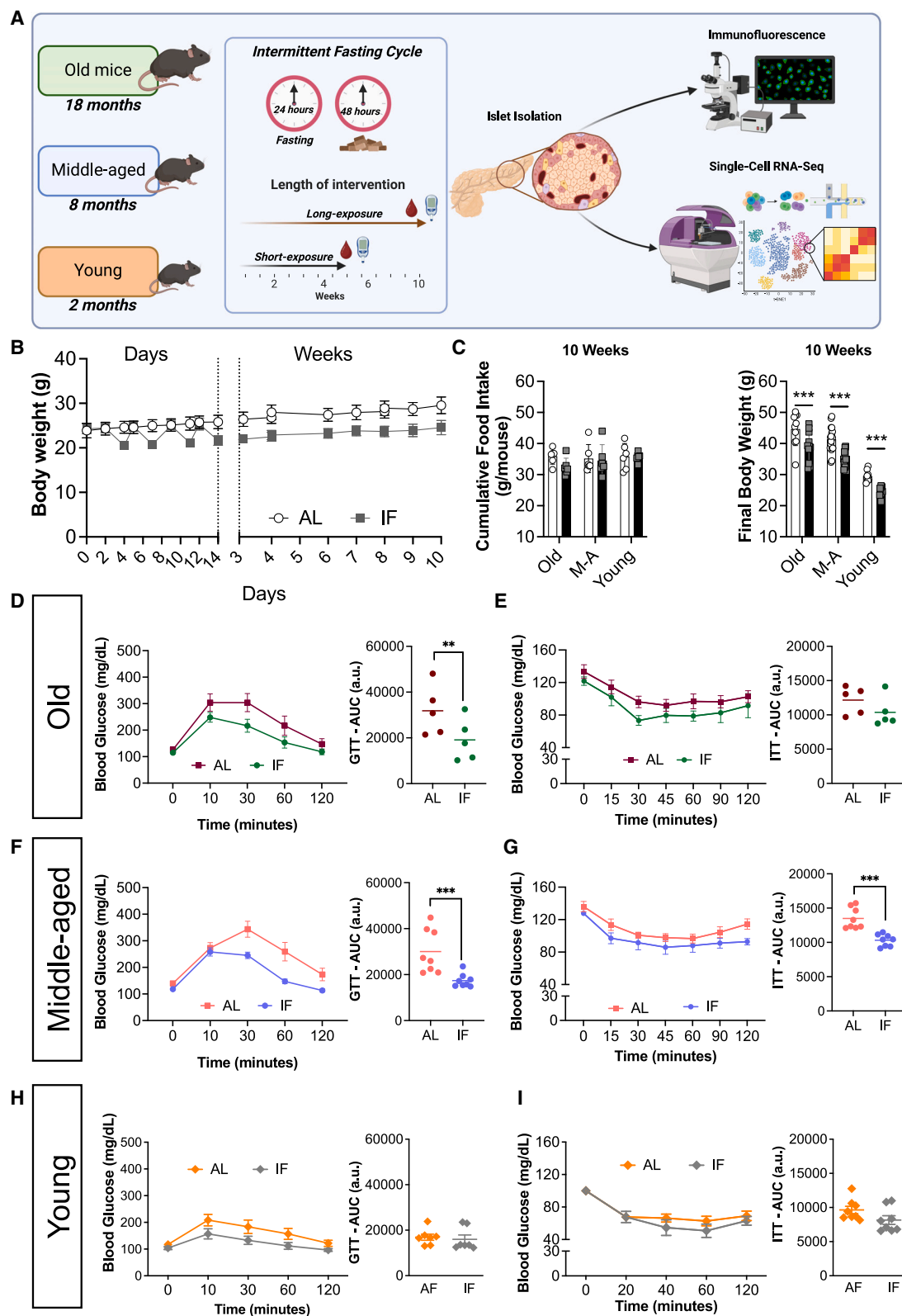
Intermittent fasting (IF) is a nutritional lifestyle intervention with broad metabolic benefits, but whether the impact of IF depends on the individual's age is unclear. Here, we investigated the effects of IF on systemic metabolism and  $\beta$  cell function in old, middle-aged, and young mice. Short-term IF improves glucose homeostasis across all age groups without altering islet function and morphology. In contrast, while chronic IF is beneficial for adult mice, it results in impaired  $\beta$  cell function in the young. Using single-cell RNA sequencing (scRNA-seq), we delineate that the  $\beta$  cell maturation and function scores are reduced in young mice. In human islets, a similar pattern is observed in type 1 (T1D), but not type 2 (T2D), diabetes, suggesting that the impact of chronic IF in adolescence is linked to the development of  $\beta$  cell dysfunction. Our study suggests considering the duration of IF in younger persons, as it may worsen rather than reduce diabetes outcomes.

## INTRODUCTION

Modern nutritional habits are characterized by an overconsumption of energy-dense and palatable foods, typically rich in lipids and carbohydrates. This positive energy balance is associated with the development of obesity and related comorbidities such as diabetes, cardiovascular disease, and cancer.<sup>1</sup> Several nutritional strategies have been explored to prevent weight gain, induce weight loss, and counteract obesity-related diseases to improve metabolic health. Intermittent fasting (IF), a dietary strategy that alternates between periods of fasting and eating, has gained popularity over the past decade. Most human studies suggest that a fasting period of at least 10 h, followed by an eating window for the remainder of the day, is necessary for any metabolic benefits.<sup>2</sup> In mice, alternating between 1 fasting day and 2 feeding days leads to improvements in glucose homeostasis that are largely independent of changes in body weight.<sup>3</sup> Most IF strategies have been proven to exert beneficial effects on metabolic parameters in humans and experimental mouse models, including body weight, insulin sensitivity, plasma cholesterol profiles, blood pressure, and lifespan.<sup>4–8</sup> The systemic beneficial effects of IF stem from molec-

ular effects on the cellular level in several tissues. During fasting-feeding cycles, the nutrient flux between tissues and cells is stimulated, triggering diverse adaptive responses, including the clearance of potentially detrimental cellular waste. During feeding periods, elevated glucose and insulin levels activate pathways associated with protein synthesis and cell growth, driving cell proliferation and organelle synthesis. Conversely, during fasting, reduced plasma insulin and glucose levels increase cellular energetic stress,<sup>9</sup> which is associated with enhanced cellular turnover and autophagy.<sup>10–12</sup> IF, by reducing cellular glucose flux, decreases adenosine triphosphate (ATP) intracellular levels and increases adenosine monophosphate (AMP). The increase in AMP activates AMP kinase (AMPK), a sensor of lower energy levels, which also activates PPAR $\gamma$  coactivator 1- $\alpha$  (PGC1- $\alpha$ ), stimulating mitochondrial biogenesis and function.<sup>13–15</sup> Enhanced redox homeostasis helps to neutralize reactive oxygen species (ROS), which prevents oxidative stress, cell dysfunction, inflammation, and, chronically, cell death.<sup>16,17</sup> These beneficial responses have been implicated in the management of diabetes. Type 2 diabetes (T2D), formerly also known as adult-onset diabetes, is characterized by insulin resistance in the periphery, impaired  $\beta$  cell function,





(legend on next page)

and hyperglycemia. T2D is associated with  $\beta$  cell mitochondrial dysfunction, oxidative stress, and inflammation.<sup>18,19</sup> Also, it is associated with blunted growth and proliferative capacity of  $\beta$  cells and ultimately results in cell death and loss of  $\beta$  cell mass.<sup>13</sup> Likewise, type 1 diabetes (T1D), also referred to as juvenile diabetes, is defined as an autoimmune response that leads to loss of  $\beta$  cell function and mass.<sup>17</sup> A dysfunctional stress response induced by autoimmune attack and/or viral infection contributes to cell death. In the endoplasmic reticulum (ER), for example, viral infections or inflammatory cytokines induce the accumulation of misfolded proteins and cause ER stress.<sup>20</sup> The pro-inflammatory response is also correlated with mitochondrial impairment and oxidative stress.<sup>21</sup> However, due to the inability of  $\beta$  cells to properly regenerate, patients with T1D display atrophy of  $\beta$  cells, lower or no levels of intracellular insulin content, and small, highly inflamed islets.<sup>22</sup> In the context of T2D, IF is associated with increased expression of insulin synthesis and secretion genes, increased insulin content, and improved  $\beta$  cell function.<sup>23</sup> Besides that, it has been shown that IF protects  $\beta$  cells by improving antioxidant capacity, decreasing ROS formation, and positively modulating the immune system response to counteract inflammation.<sup>23–26</sup> In contrast, the effects of IF on T1D are largely unclear. Considering that IF promotes tissue regeneration, it is possible that IF influences  $\beta$  cell dysfunction and death. It has been speculated that IF could provide auxiliary support for individuals with T1D by reducing the need for exogenous insulin. A review of prior studies suggests that fasting in T1D has potential beneficial outcomes when adjustments to insulin are properly managed to support glycemic control.<sup>27</sup> In summary, IF has been proven effective in clinical and pre-clinical settings to counteract metabolic dysfunction observed in T2D and islet dysfunction. However, data on very young and very old subjects are scarce, even though previous studies reported that the effects of dietary restriction on body weight and lifespan are dependent on the genetic makeup and age of initiation.<sup>28</sup> We hypothesize that IF could impact whole-body glucose metabolism, as well as islet function and capacity, in an age-dependent manner. To address these hypotheses, we employed a combination of immunofluorescence, isolated islets assay, and single-cell RNA sequencing (scRNA-seq) approaches to analyze the effect of IF on glucose homeostasis in mice at various life stages.

## RESULTS

### Beneficial metabolic effects of IF in an age-independent manner

IF is a lifestyle intervention that follows various modalities from days to weeks or months. To evaluate the short-term (ST) vs. long-term (LT) effects on metabolic homeostasis and  $\beta$  cell func-

tion, we evaluated the effects of 5 (ST) and 10 weeks (LT) IF on body weight and food intake of 2-month-old (young), 8-month-old (middle-aged), and 18-month-old (old) wild-type mice (Figure 1A) compared to age-matched control groups fed *ad libitum*. We observed that during the ST-IF intervention, old and middle-aged mice did not display changes in body weight (Figures S1A, S1B, S1F, and S1G). In the young group on ST-IF, we observed lower body weights, which was linked to lower food intake compared to the young *ad libitum* control group (Figures S1K and S1L). Furthermore, independent of their age, all groups exposed to the LT-IF intervention displayed lower body weights compared to their respective age control *ad libitum* groups (Figures 1B and 1C), while food intake remained unchanged (Figures S1B and S1G). It is well established that IF has beneficial effects on insulin sensitivity and glucose homeostasis even independently of weight loss.<sup>4</sup> To this end, we performed dynamic glucose tolerance tests (GTTs) and insulin tolerance tests (ITTs). At the end of the ST-IF intervention, compared to the *ad libitum* controls, the IF groups exhibited age-independent improvements in both GTTs and ITTs (Figures S1C, S1D, S1H–S1J, S1M, and S1N). Taken together, these results indicate that ST-IF improved glucose homeostasis and insulin sensitivity independently of age. As the ST-IF intervention improved glucose and insulin tolerance, we monitored if these IF-induced adaptations were sustained in the LT. In old mice subjected to LT-IF, GTT was improved compared to the control *ad libitum* group (Figure 1D). In contrast, the ITT of the LT-IF mice did not differ from the *ad libitum* group (Figure 1E). In middle-aged mice, in comparison to the *ad libitum* group, LT-IF improved both GTTs and ITTs (Figures 1F and 1G). To our surprise, the GTTs and ITTs of young mice were indifferent between the LT-IF and *ad libitum* groups (Figures 1H and 1I).

### LT-IF impairs $\beta$ cells function in younger mice

As one benefit of IF is linked to the endocrine pancreas, we hypothesized that the absence of LT-IF benefits in young mice was potentially linked to  $\beta$  cells. While we did not find any difference in pancreas weights between the *ad libitum* and LT-IF groups, independently of age (Figures S1E, S1J, and S1O), we investigated islet and  $\beta$  cell function further. In isolated primary islets, we performed glucose-stimulated insulin secretion (GSIS) tests to directly assess  $\beta$  cell function. At low glucose concentrations, islets from the LT-IF and *ad libitum* groups secreted comparable insulin levels. However, islets isolated from old LT-IF mice secreted more insulin in response to high glucose than islets isolated from the old *ad libitum* group (Figure 2A), indicating a beneficial effect of IF on GSIS, while no significant changes were observed in islets isolated from the middle-aged mice (Figure 2B). Contrary to this, islets isolated from young mice after LT-IF showed lower GSIS compared to the control *ad libitum* group

**Figure 1. Long-term IF improves glucose homeostasis in middle-aged and old mice but not in young mice**

(A) Study design from mice *in vivo* and *ex vivo* procedures (A).

(B) Young body weight expressed in days and weeks.

(C) Cumulative food intake and final body weight after 10 weeks of IF intervention.

(D–I) Glucose (2.5 mg/kg) and insulin (0.8 U/kg) tolerance tests executed after 10 weeks of IF in old (D and E, respectively), middle-aged (F and G), and young mice (H and I).

AL, *ad libitum*; IF, intermittent fasting; GTT, glucose tolerance test; ITT, insulin tolerance test; AUC, area under curve. Data are expressed as mean  $\pm$  standard error of the mean (old:  $n = 5$ /group; middle aged:  $n = 8$ /group; young mice:  $n = 9$ /group). Statistical differences: \*\* $p < 0.01$  and \*\*\* $p < 0.001$ .



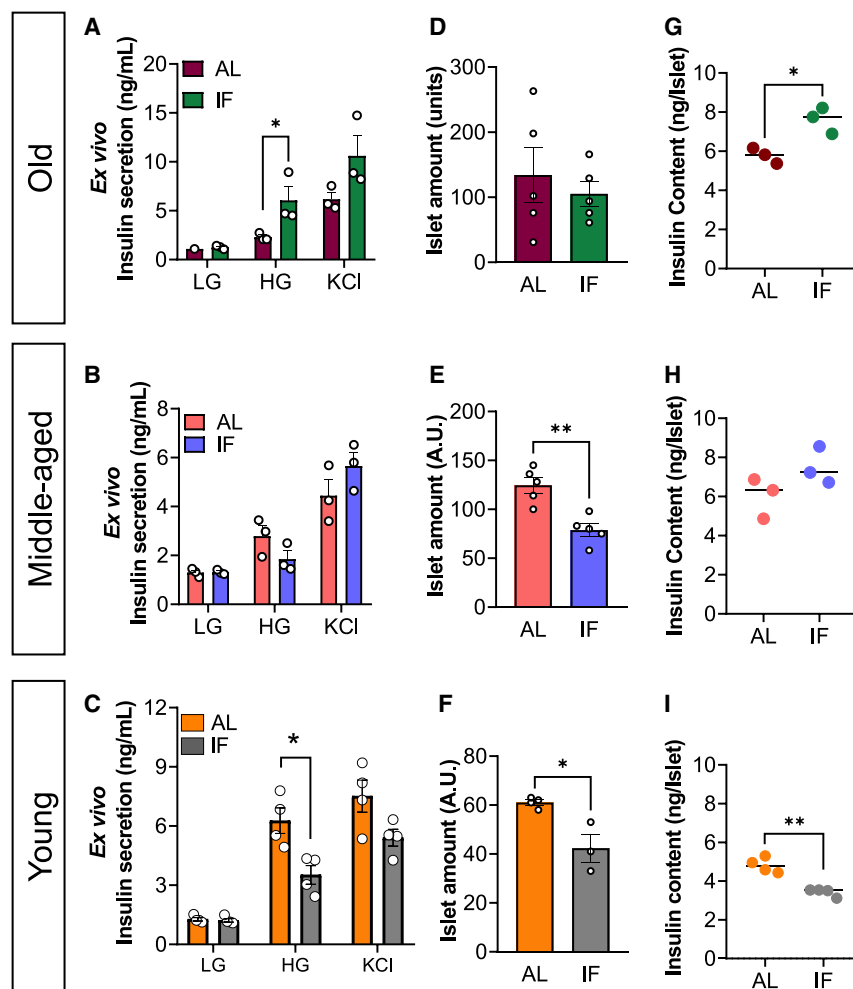


**Figure 2. Long-term IF increases insulin content and secretion in old mice but decreases them in young mice**

Ex vivo insulin secretion, islet amount, and insulin content after 10 weeks of IF in old mice (A, D, and G), middle-aged (B, E, and H), and young mice (C, F, and I). AL, *ad libitum*; IF, intermittent fasting. Data are expressed as mean  $\pm$  standard error of the mean (old:  $n = 3$ /group; middle aged:  $n = 3$ /group; young mice:  $n = 4$ /group) for islet amount measurement (old:  $n = 4$ /group; middle aged:  $n = 5$  *ad libitum* group and 4 IF group; young mice:  $n = 3$ /group). Statistical differences: \* $p < 0.05$  and \*\* $p < 0.01$ .

10 weeks of IF. By immunofluorescence, we observed that although there was no difference in islet area (sum of  $\beta$  and  $\alpha$  cell populations and nuclei) (Figures 3A and 3B), islets in young mice subjected to LT-IF had lower  $\alpha$  (Figure 3C) and  $\beta$  cell (Figure 3D) and  $\alpha/\beta$  cell ratios compared to the *ad libitum* group (Figure 3E). Additionally, we observed that LT-IF was associated with less BrdU<sup>+</sup> labeling in insulin- and glucagon-positive cells, pointing to reduced proliferation of both  $\alpha$  and  $\beta$  cells (Figures 3F and 3G). In old mice, the quantification for insulin- and glucagon-positive cells indicated that compared to the *ad libitum* control group, islets from LT-IF had lower  $\alpha$  cell mass (Figures S2A–S2C). However, islet area,  $\beta$  cell, BrdU-positive insulin, and glucagon-positive cells were indifferent between the *ad libitum* and LT-IF groups in old mice (Figures S2B–S2G).

(Figure 2C). Maximal secretion capacity, as assessed by KCl-induced insulin secretion, was indifferent in any group, although it followed the pattern observed for GSIS (i.e., a trend toward higher secretion in old and lower secretion in young IF mice) (Figures 2A–2C). To explore the mechanism of these age-dependent effects of LT-IF on insulin secretion, we quantified islet amount and insulin content. Interestingly, the islet quantity was unchanged in the old mice (Figure 2D) but lower in the middle-aged (Figure 2E) and young LT-IF groups compared to their *ad libitum* controls (Figure 2F). The insulin content of isolated islets was higher in the old (Figure 2G), did not change in the middle-aged (Figure 2H), and was lower in the young LT-IF groups (Figure 2I) compared to their *ad libitum* control groups. Altogether, our data indicated that LT-IF improved ex vivo islet function in old mice and impaired islet function in adolescent mice.

### Impaired islet function is linked to lower $\alpha$ and $\beta$ cell mass and proliferation

Based on the impaired islet function after LT-IF in young mice, we next investigated whether IF affected  $\alpha$  and  $\beta$  cell masses and proliferation. Mice were injected with BrdU<sup>+</sup> for 5 days after

In middle-aged mice, no significant changes in islet area,  $\alpha$  and  $\beta$  cell mass,  $\alpha/\beta$  cell mass ratio, or  $\alpha$  and  $\beta$  cell proliferation staining were observed between the groups (Figures S2H–S2N). Together, our data suggest that in young mice, LT-IF impaired  $\alpha$  and  $\beta$  cell proliferation, contributing to reduced islet function and insulin secretion. However, this was not seen in old and middle-aged mice.

### Islet scRNA-seq reveals altered $\beta$ cell maturation and function in young LT-IF mice

In old mice, LT-IF was associated with enhanced  $\beta$  cell function but was impaired in young mice compared to their *ad libitum* controls. To unravel the underlying differences in function and cell populations, we performed scRNA-seq of isolated islets from young, middle-aged, and old mice after LT-IF. From the expression matrix with cells as columns and genes as rows, we assigned cell clusters to the main endocrine cell types based on the established marker genes *Gcg* (glucagon found in  $\alpha$  cells), *Ins1* (insulin found in  $\beta$  cells), *Ppy* (pancreatic polypeptide found in pancreatic polypeptide cells), and *Sst* (somatostatin in  $\delta$  cells) (Figure S3B). After duplex removal of the main endocrine cell types, we distinguished distinct *Gcg*-, *Ins1*-, *Ppy*-, and *Sst*-

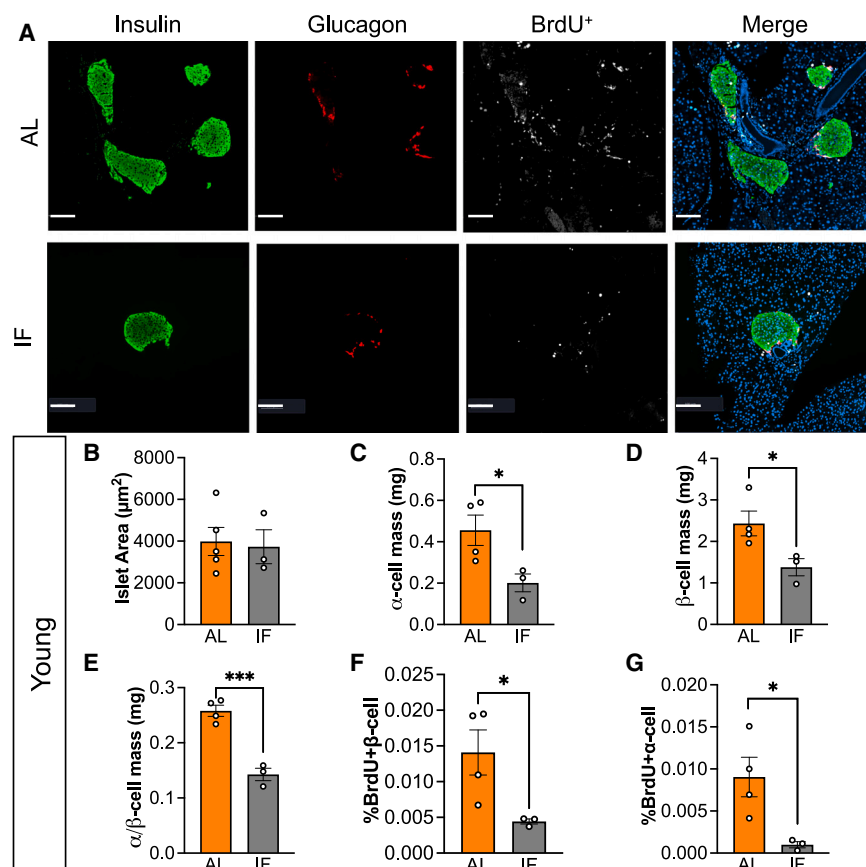


**Figure 3. Lower insulin secretion and content in young IF mice are associated with reduced islet numbers and impaired  $\alpha$  and  $\beta$  cell proliferative capacity**

(A) Immunofluorescence from islets from young mice after long-term IF. (B–G) Islet area  $\mu\text{m}^2$  (B),  $\alpha$  cell mass (C),  $\beta$  cell mass (D),  $\alpha$  and  $\beta$  cell ratio (E),  $\alpha$  and  $\beta$  cell mass, and percentage of BrdU+  $\alpha$  (F) and  $\beta$  (G) cell proliferation. Insulin+ cells: green; glucagon+ cells: red; BrdU+ cells: white; nuclear staining (DAPI): blue. (A) Scale bar: 100  $\mu\text{m}$ . AL, *ad libitum*; IF, intermittent fasting. Data are expressed as mean  $\pm$  standard error of the mean ( $n = 4$  in the *ad libitum* group and 3 in the IF group). Statistical differences: \* $p < 0.05$ , \*\* $p < 0.01$ , and \*\*\* $p < 0.001$ .

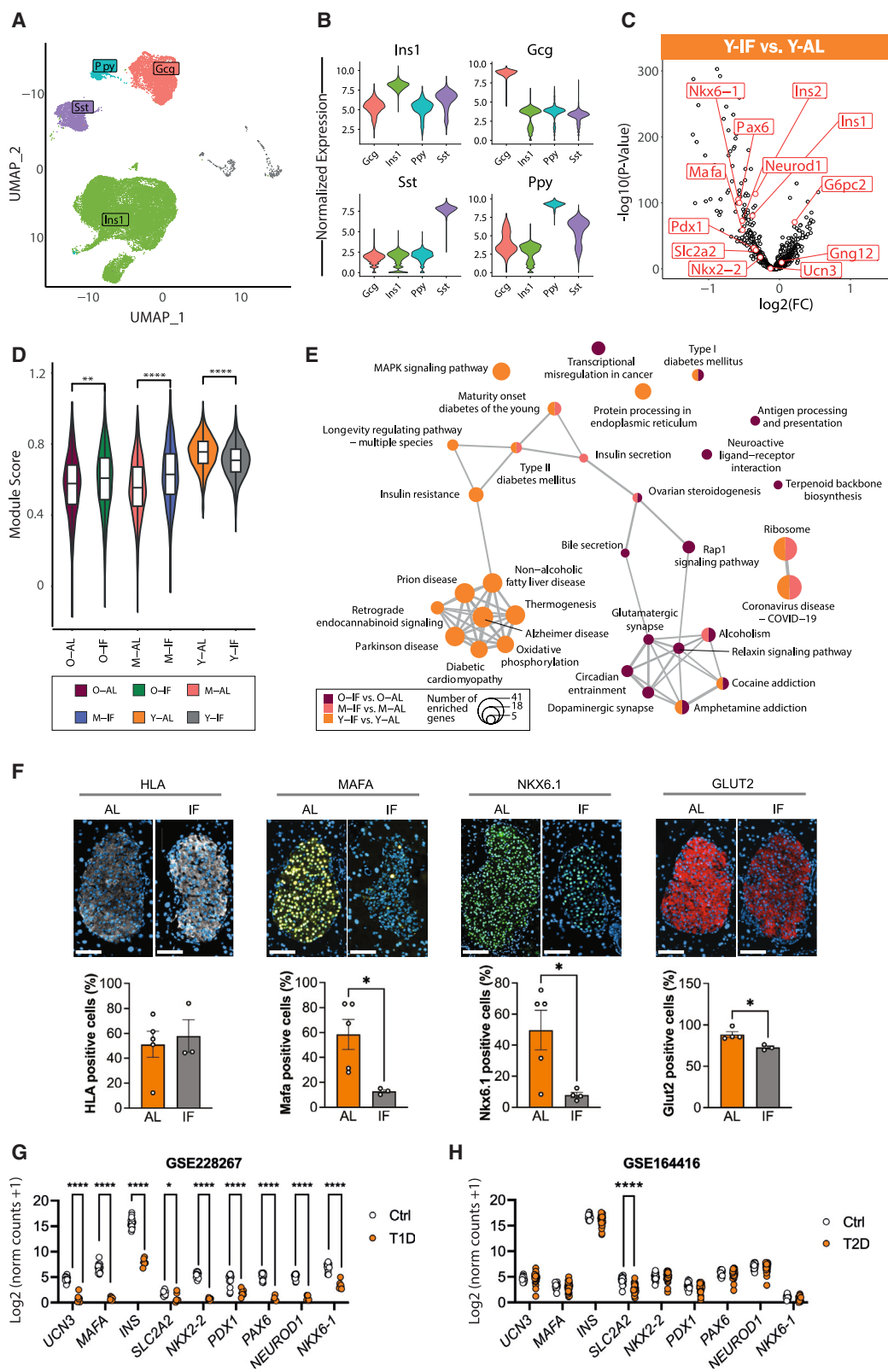
candidate genes, as highlighted in volcano plots (Figures 4C, S3D, and S3E) and visualized as a heatmap (Figure S3H). Most of these candidate genes, such as *Mafa*, *Nkx-6-1*, *Slc2a2*, and *Ins1*, were lower only in young mice subjected to LT-IF compared to *ad libitum* but not in middle-aged or old mice (Figure S3H). To verify if the transcriptional changes also translated into protein levels, we quantified the expression of the significantly reduced candidates by histoimmunofluorescence and observed lower expression of MAFA, GLUT2, and

positive cell populations (Figures 4A and 4B). In addition, we found the expected non-endocrine cell types, confirming the validity of our scRNA-seq approach (Figure S3C). Further unsupervised cell clustering from the whole dataset revealed 22 sub-cell populations (Figure S3A). We focused our bioinformatic analyses on  $\beta$  cells to determine age- and IF-dependent transcriptomic responses (Figures 4C, S3D, and S4E; Table S1) and performed a quantitative analysis of islet-specific biological programs described in the literature,<sup>26</sup> which were augmented with custom gene sets (Table S1). Module scores based on those programs resemble features that can be interpreted functionally and are tailored to the specific biological context in question. We found that the most significant difference between *ad libitum* and LT-IF groups was the “ $\beta$  cell maturation” gene set (Figures 4D and S3G; Table S2). Whereas in old and middle-aged mice,  $\beta$  cell maturation scores were higher after LT-IF, they were lower in young mice compared to their *ad libitum* controls (Figure 4D). Also, when we stratified this analysis by heterogeneous  $\beta$  cell clusters, we found the same effects in all clusters (Figure S3G). We also investigated the overrepresentation of KEGG pathways in the differentially regulated genes of  $\beta$  cells (Table S3). We identified a cluster of related KEGG pathways that included pathways for T2D and insulin function (Figures 4E and S3F; Table S4). We used the overlap of genes annotated to the  $\beta$  cell maturation program with those contributing to any pathway overrepresentation of the found clusters to identify possible

NKX6.1 proteins in the LT-IF young group compared to the young controls (Figure 4F). HLA, a marker of inflammation, tended to be lower in the aged group, but no alteration was found in the middle-aged mice (Figures S4A and S4B). Next, we examined the relevance of the candidate markers in human data by analyzing published bulk RNA-seq datasets from human islets of donors with T1D and T2D and observed that the genes specifically downregulated in the LT-IF young group exhibited a similar pattern of downregulation in samples from patients with T1D samples but not in T2D samples (Figures 4G and 4H).

## DISCUSSION

Despite the existing evidence of the beneficial effects of IF on metabolic health, if these apply to all life stages remains largely unexplored. Most IF studies were understandably conducted in adult humans or middle-aged/elderly mice, as these demographics are at higher disease risk compared to the young. Still, there is limited knowledge about the impact of IF on younger populations.<sup>29</sup> In this study, we investigated the impact of age on IF-induced improvements in glucose homeostasis. We found that while ST-IF had metabolic benefits across all tested age groups, LT-IF negatively impacted  $\beta$  cell function only in young mice. Using scRNA-seq of isolated islets, we discovered a transcriptional profile linked to impaired  $\beta$  cell maturation specifically



(legend on next page)

in the young. Further bioinformatic analysis revealed that this was linked to a transcriptional signature of  $\beta$  cell maturation and function-related genes observed in humans with T1D. Overall, our data align well with previous findings, demonstrating that a short IF regimen enhances insulin sensitivity.<sup>4,5,10</sup> The finding that longer IF periods may also have deleterious consequences is a novel finding with relevant implications, especially for using IF in adolescents and people at high T1D risk. Previous studies have reported that a fine balance in nutrient flux is necessary for tissue maturation and function, and fasting interventions in immature mice may trigger metabolic impairment. In agreement with our findings, Yin et al. demonstrated that 12 weeks of IF intervention in pregnant mice predisposes their offspring to liver steatosis and adiposity, suggesting that IF should be avoided during pregnancy due to its potential adverse effects on fetal development and offspring metabolic homeostasis.<sup>30</sup> Bayliah et al. found that while IF had beneficial effects on redox homeostasis and energy metabolism in the older groups, it appeared to decrease antioxidant capacity in the cortex of young mice.<sup>31</sup> These findings align with the results from Jianghua et al., which showed that IF affects brain energy metabolism by reducing brain insulin signaling and, consequently, peripheral insulin production and secretion.<sup>32</sup> Previous studies also indicate a potential impairment induced by LT-IF interventions. In light of our study, this supports the notion that during the period of development and maturation, IF might impair proper nutrient flux and hormonal balance required for proper cell differentiation and organ development. The young mice displayed reduced  $\alpha$  and  $\beta$  cell mass after LT-IF, which was not observed in the middle-aged or old mice. A reduction in cellular nutrient flux may lead to an atrophic cellular remodeling. Atrophic responses are generally associated with secretory malfunction,<sup>33,34</sup> an early indication of  $\beta$  cell failure,<sup>26,29</sup> including altered pro-insulin processing, elevated pro-insulin levels, a reduction in secretory granules, and  $\beta$  cell deterioration.<sup>34,35</sup> These pathological responses can be triggered by genetic predisposition (lowered secretory capacity) and environmental stressors. Imbalances in calcium, redox, or mitochondrial homeostasis lead to a pro-oxidative and -inflammatory environment and, in later stages, to  $\beta$  cell apoptosis.<sup>36</sup> Furthermore, suboptimal nutrient flux may contribute to impaired cellular maintenance and development.<sup>37</sup> Although the direct effects of these factors remain unclear, it might very well be related to the deleterious effect of IF observed in our study.<sup>32</sup> An interesting finding was that IF prevented the age-related decline in GSIS. This decline in insulin secretion has been widely reported in the literature and is a hall-

mark of aging, which underscores the importance of IF as a preventative strategy against diabetes. In aging, mTORC1 activity plays a critical role in  $\beta$  cells being associated with increased cellular stress and impaired function. Although mTORC1 activation is protective in younger individuals, it becomes deleterious with age. IF has been shown to modulate mTORC1 activity, thereby potentially mitigating the adverse effects of aging on insulin secretion and maintaining metabolic health in older populations,<sup>38</sup> as observed in the present study. Regarding the young mice, our scRNA-seq analyses revealed that LT-IF led to a distinct molecular signature characterized by lower expression of, e.g., *Mafa*, *Nkx6-1*, *Slc2a2*, and *Ins1*, which was confirmed by histoimmunofluorescence analysis. These are important markers for glucose transport, insulin synthesis, and secretion, suggesting that LT-IF may adversely impact  $\beta$  cell maturation and function. To explore the expression of the genes in humans in T1D and T2D, we analyzed public bulk RNA-seq datasets from donors with T1D and T2D. While we observed similar downregulation patterns of key  $\beta$  cell genes in T1D samples, we recognize that bulk RNA-seq data do not allow us to distinguish between decreased  $\beta$  cell numbers and reduced gene expression within individual  $\beta$  cells. As T1D samples naturally have fewer  $\beta$  cells, the observed decreases may reflect a reduced  $\beta$  cell population rather than intrinsic changes in gene expression. Despite this limitation, this suggests potential parallels between the impact of LT-IF in young mice and  $\beta$  cell dysfunction in humans with T1D, which was not observed in T2D, even though the islet dedifferentiation process is likely present. Our findings discover a vulnerability of developing  $\beta$  cells to extended fasting periods. This is particularly relevant considering the growing popularity of IF across diverse age groups. Further research is needed to determine how these findings translate to conditions where obesity is the primary driver of islet dysfunction or in autoimmune models of T1D such as non-obese diabetic (NOD) mice. In conclusion, our study underscores the importance of tailored approaches in dietary practices and highlights the need for comprehensive longitudinal studies to elucidate the LT effects of IF, particularly in human populations and individuals with a predisposition to diabetes. While IF exhibits promising metabolic benefits in the ST, the potential age-dependent adverse effects observed with prolonged fasting require more attention and caution.

### Limitations of the study

This study provides valuable insights into the age-dependent effects of IF on glucose metabolism and  $\beta$  cell function in mice. Our

### Figure 4. scRNA-seq reveals impaired $\beta$ cell maturation and development in young mice

(A and B) Uniform manifold approximation and projection (UMAP) of whole dataset after duplex removal with color-coded endocrine cell types; labels show main marker genes (A), and violin plots show the expression of marker genes in the identified cell types (B).  
(C) Differential gene expression is visualized as a volcano plot with biological effect size ( $\log_2$  fold change [ $\log_2(\text{FC})$ ]) on the x axis and statistical significance ( $-\log_{10}(p \text{ value})$ ) on the y axis (C).  
(D) Comparison of module scores for  $\beta$  cell maturation markers between IF and *ad libitum* in all age groups. Overrepresentation of KEGG pathways from differentially expressed gene colors indicates contrasts in which significant results were found: IF vs. *ad libitum* group in old (O-IF vs. O-AL), middle-aged (M-IF vs. M-AL), and young mice (Y-IF vs. Y-AL).  
(E) Connected clusters are based on semantic similarity and size of nodes indicate several genes.  
(F) Immunofluorescence for HLA, MAFA, NKX6.1, and GLUT 2. Scale bar: 50  $\mu\text{m}$ .  
(G and H) RNA-seq of isolated  $\beta$  cells from human donors with type 1 diabetes (G) or type 1 diabetes (H). Statistical significance: \**padj* < 0.05, \*\**padj* < 0.01, \*\*\**padj* < 0.001, and \*\*\*\**padj* < 0.0001.



findings are primarily derived from a mouse model, which, despite its usefulness in pre-clinical research, cannot completely emulate human metabolic processes. Another limitation is the use of only male mice, which may limit the generalizability of our findings to females. The age classifications used correspond to mouse physiology and may not translate directly to human life stages, where developmental and metabolic processes differ significantly. *In vivo* insulin secretion was not measured, which would have provided additional insights. Besides that, we measured pooled pancreatic islets, and biological replicates should be sequenced independently and treated as pseudo-bulks in statistics. Future studies should address these limitations by including a more diverse set of physiological models, addressing sexual differences and behavioral endpoints.

## RESOURCE AVAILABILITY

### Lead contact

Requests for further information and resources should be directed to and will be fulfilled by the lead contact, Prof. Dr. Stephan Herzig ([stephan.herzig@helmholtz-muenchen.de](mailto:stephan.herzig@helmholtz-muenchen.de)).

### Materials availability

This study did not generate new unique reagents.

### Data and code availability

scRNA-seq data have been deposited at NCBI GEO: GSE275356. Any additional information required to reanalyze the data reported in this paper is available from the lead contact upon request.

## ACKNOWLEDGMENTS

We thank all lab members. S.H. was supported by the/ Helmholtz Future Topic AMPPro. A.B. was supported by DFG (SFB1123-B10 and SPP2306 BA4925/2-1), the Deutsches Zentrum für Herz-Kreislaufforschung (DZHK), and the European Research Training Group (ERC) Starting Grant PROTEOFIT. M.R. is funded by the European Research Council (ERC) under the European Union's Horizon 2020 research and innovation program (#949017) and the German Diabetes Center (DZD) Next grant. We acknowledge BioRender.com for help with the figures.

## AUTHOR CONTRIBUTIONS

Conceptualization, L.M., P.W., S.E., M.R., A.B., and S.H.; data curation, L.M., P.W., S.E., J.G., M.R., M.S., and H.L.; analysis, L.M., P.W., S.E., J.G., M.R., M.S., and H.L.; visualization, L.M., P.W., S.E., A.W.-H., D.H., L.K.B., K.K., J.S., J.G., M.R., M.S., and H.L.; writing, A.B., L.M., P.W., A.W.-H., D.H., J.G., and S.H.; methodology, P.W., S.E., A.W.-H., D.H., L.K.B., K.K., J.S., J.G., M.R., M.S., and H.L.; investigation, S.E., A.W.-H., D.H., L.K.B., K.K., J.S., and M.R.; review, S.E., L.K.B., K.K., J.S., M.R., M.S., and H.L.; administration, S.E., M.R., A.B., and S.H.; supervision, A.B. and S.H.; funding acquisition, S.H.

## DECLARATION OF INTERESTS

All authors declare that they have no competing interests.

## STAR★METHODS

Detailed methods are provided in the online version of this paper and include the following:

- **KEY RESOURCES TABLE**
- **EXPERIMENTAL MODEL AND STUDY PARTICIPANT DETAILS**
  - Mouse model

## METHOD DETAILS

- Intermittent fasting
- Glucose tolerance tests (GTT) and insulin tolerance tests (ITT)
- Islet isolation
- Insulin secretion and content assay
- Immunofluorescence
- BrdU incorporation and detection
- Single-cell RNA-Sequencing sample preparation and data Generation
- ScRNA-seq data processing, quality control, and analysis
- Gene Expression Omnibus data collection and analysis
- Statistical analysis

## SUPPLEMENTAL INFORMATION

Supplemental information can be found online at <https://doi.org/10.1016/j.celrep.2024.115225>.

Received: June 19, 2024

Revised: December 1, 2024

Accepted: December 29, 2024

Published: January 18, 2025

## REFERENCES

1. Chew, N.W.S., Ng, C.H., Tan, D.J.H., Kong, G., Lin, C., Chin, Y.H., Lim, W.H., Huang, D.Q., Quek, J., Fu, C.E., et al. (2023). The global burden of metabolic disease: Data from 2000 to 2019. *Cell Metabol.* 35, 414–428.e3. <https://doi.org/10.1016/j.cmet.2023.02.003>.
2. Welton, S., Minty, R., O'Driscoll, T., Willms, H., Poirier, D., Madden, S., and Kelly, L. (2020). Intermittent fasting and weight loss: Systematic review. *Can. Fam. Physician* 66, 117–125.
3. de Cabo, R., and Mattson, M.P. (2019). Effects of Intermittent Fasting on Health, Aging, and Disease. *N. Engl. J. Med.* 381, 2541–2551. <https://doi.org/10.1056/NEJMRA1905136>.
4. Cienfuegos, S., Gabel, K., Kalam, F., Ezpeleta, M., Wiseman, E., Pavlou, V., Lin, S., Oliveira, M.L., and Varady, K.A. (2020). Effects of 4- and 6-h Time-Restricted Feeding on Weight and Cardiometabolic Health: A Randomized Controlled Trial in Adults with Obesity. *Cell Metabol.* 32, 366–378.e3. <https://doi.org/10.1016/j.cmet.2020.06.018>.
5. Schübel, R., Nattenmüller, J., Sookthai, D., Nonnenmacher, T., Graf, M.E., Riedl, L., Schlett, C.L., Von Stackelberg, O., Johnson, T., Nabers, D., et al. (2018). Effects of intermittent and continuous calorie restriction on body weight and metabolism over 50 wk: a randomized controlled trial. *Am. J. Clin. Nutr.* 108, 933–945. <https://doi.org/10.1093/AJCN/NQY196>.
6. Trepanowski, J.F., Kroeger, C.M., Barnosky, A., Klempel, M.C., Bhutani, S., Hoddy, K.K., Gabel, K., Freels, S., Rigdon, J., Rood, J., et al. (2017). Effect of Alternate-Day Fasting on Weight Loss, Weight Maintenance, and Cardioprotection Among Metabolically Healthy Obese Adults: A Randomized Clinical Trial. *JAMA Intern. Med.* 177, 930–938. <https://doi.org/10.1001/JAMAINTERNMED.2017.0936>.
7. Xie, K., Neff, F., Markert, A., Rozman, J., Aguilar-Pimentel, J.A., Amarie, O.V., Becker, L., Brommage, R., Garrett, L., Henzel, K.S., et al. (2017). Every-other-day feeding extends lifespan but fails to delay many symptoms of aging in mice. *Nat. Commun.* 8, 155. <https://doi.org/10.1038/s41467-017-00178-3>.
8. Li, G., Xie, C., Lu, S., Nichols, R.G., Tian, Y., Li, L., Patel, D., Ma, Y., Brocker, C.N., Yan, T., et al. (2017). Intermittent Fasting Promotes White Adipose Browning and Decreases Obesity by Shaping the Gut Microbiota. *Cell Metabol.* 26, 672–685.e4. <https://doi.org/10.1016/j.cmet.2017.08.019>.
9. Longo, V.D., and Mattson, M.P. (2014). Fasting: molecular mechanisms and clinical applications. *Cell Metabol.* 19, 181–192. <https://doi.org/10.1016/j.cmet.2013.12.008>.
10. Mishra, A., Mirzaei, H., Guidi, N., Vinciguerra, M., Mouton, A., Linardic, M., Rappa, F., Barone, R., Navarrete, G., Wei, M., et al. (2021). Fasting-mimicking



- diet prevents high-fat diet effect on cardiometabolic risk and lifespan. *Nat. Metab.* 3, 1342–1356. <https://doi.org/10.1038/S42255-021-00469-6>.
11. Jouandin, P., Marelja, Z., Shih, Y.H., Parkhitko, A.A., Dambowsky, M., Asara, J.M., Nemazany, I., Dibble, C.C., Simons, M., and Perrimon, N. (2022). Lysosomal cystine mobilization shapes the response of TORC1 and tissue growth to fasting. *Science* 375, eabc4203. <https://doi.org/10.1126/SCIENCE.ABC4203>.
12. Zhao, Y., Jia, M., Chen, W., and Liu, Z. (2022). The neuroprotective effects of intermittent fasting on brain aging and neurodegenerative diseases via regulating mitochondrial function. *Free Radic. Biol. Med.* 182, 206–218. <https://doi.org/10.1016/J.FREERADBIOMED.2022.02.021>.
13. Anton, S.D., Moehl, K., Donahoo, W.T., Marosi, K., Lee, S.A., Mainous, A.G., Leeuwenburgh, C., and Mattson, M.P. (2018). Flipping the Metabolic Switch: Understanding and Applying the Health Benefits of Fasting. *Obesity* 26, 254–268. <https://doi.org/10.1002/OBY.22065>.
14. Lv, C., Sun, Y., Zhang, Z.Y., Aboelela, Z., Qiu, X., and Meng, Z.X. (2022).  $\beta$ -cell dynamics in type 2 diabetes and in dietary and exercise interventions. *J. Mol. Cell Biol.* 14, mjac046. <https://doi.org/10.1093/JMCB/MJAC046>.
15. Harney, D.J., Cielesh, M., Chu, R., Cooke, K.C., James, D.E., Stöckli, J., and Larance, M. (2021). Proteomics analysis of adipose depots after intermittent fasting reveals visceral fat preservation mechanisms. *Cell Rep.* 34, 108804. <https://doi.org/10.1016/j.celrep.2021.108804>.
16. Zingg, J.M., Vlad, A., and Ricciarelli, R. (2021). Oxidized LDLs as Signaling Molecules. *Antioxidants* 10, 1184. <https://doi.org/10.3390/ANTIOX10081184>.
17. Hatchwell, L., Harney, D.J., Cielesh, M., Young, K., Koay, Y.C., O'Sullivan, J.F., and Larance, M. (2020). Multi-omics Analysis of the Intermittent Fasting Response in Mice Identifies an Unexpected Role for HNF4 $\alpha$ . *Cell Rep.* 30, 3566–3582.e4. <https://doi.org/10.1016/j.celrep.2020.02.051>.
18. Liu, S., Zhang, R., Zhang, L., Yang, A., Guo, Y., Jiang, L., Wang, H., Xu, S., and Zhou, H. (2024). Oxidative stress suppresses PHB2-mediated mitophagy in  $\beta$ -cells via the Nrf2/PHB2 pathway. *J. Diabetes Investig.* 15, 559–571. <https://doi.org/10.1111/JDI.14147>.
19. Dlodla, P.V., Mabhidia, S.E., Ziqubu, K., Nkambule, B.B., Mazibuko-Mbeje, S.E., Hanser, S., Basson, A.K., Pfeiffer, C., and Kengne, A.P. (2023). Pancreatic  $\beta$ -cell dysfunction in type 2 diabetes: Implications of inflammation and oxidative stress. *World J. Diabetes* 14, 130–146. <https://doi.org/10.4239/WJD.V14.I3.130>.
20. Engin, F., Yermalovich, A., Ngyuen, T., Hummasti, S., Fu, W., Eizirik, D.L., Mathis, D., and Hotamisligil, G.S. (2013). Restoration of the unfolded protein response in pancreatic  $\beta$  cells protects mice against type 1 diabetes. *Sci. Transl. Med.* 5. <https://doi.org/10.1126/SCITRANSLMED.3006534>.
21. Eguchi, N., Vaziri, N.D., Dafoe, D.C., and Ichii, H. (2021). The Role of Oxidative Stress in Pancreatic  $\beta$  Cell Dysfunction in Diabetes. *Int. J. Mol. Sci.* 22, 1509–1518. <https://doi.org/10.3390/IJMS22041509>.
22. Roep, B.O., Thomaidou, S., van Tienhoven, R., and Zaldumbide, A. (2021). Type 1 diabetes mellitus as a disease of the  $\beta$ -cell (do not blame the immune system?). *Nat. Rev. Endocrinol.* 17, 150–161. <https://doi.org/10.1038/S41574-020-00443-4>.
23. Patel, S., Yan, Z., and Remedi, M.S. (2024). Intermittent fasting protects  $\beta$ -cell identity and function in a type-2 diabetes model. *Metabolism* 153, 155813. <https://doi.org/10.1016/J.METABOL.2024.155813>.
24. Zenz, G., Jačan, A., Reichmann, F., Farzi, A., and Holzer, P. (2019). Intermittent Fasting Exacerbates the Acute Immune and Behavioral Sickness Response to the Viral Mimic Poly(I:C) in Mice. *Front. Neurosci.* 13. <https://doi.org/10.3389/fnins.2019.00359>.
25. Hrovatin, K., Bastidas-Ponce, A., Bakhti, M., Zappia, L., Büttner, M., Salinno, C., Sterr, M., Böttcher, A., Migliorini, A., Lickert, H., and Theis, F.J. (2023). Delineating mouse  $\beta$ -cell identity during lifetime and in diabetes with a single cell atlas. *Nat. Metab.* 5, 1615–1637. <https://doi.org/10.1038/S42255-023-00876-X>.
26. Harney, D.J., Cielesh, M., Roberts, G.E., Vila, I.K., Viengkhou, B., Hofer, M.J., Laguet, N., and Larance, M. (2023). Dietary restriction induces a sexually dimorphic type I interferon response in mice with gene-environment interactions. *Cell Rep.* 42, 112559. <https://doi.org/10.1016/j.celrep.2023.112559>.
27. Herz, D., Haupt, S., Zimmer, R.T., Wachsmuth, N.B., Schierbauer, J., Zimmermann, P., Voit, T., Thurm, U., Khoramipour, K., Rilstone, S., and Moser, O. (2023). Efficacy of Fasting in Type 1 and Type 2 Diabetes Mellitus: A Narrative Review. *Nutrients* 15, 3525. <https://doi.org/10.3390/NU15163525>.
28. Goodrick, C.L., Ingram, D.K., Reynolds, M.A., Freeman, J.R., and Cider, N. (1990). Effects of intermittent feeding upon body weight and lifespan in inbred mice: interaction of genotype and age. *Mech. Ageing Dev.* 55, 69–87. [https://doi.org/10.1016/0047-6374\(90\)90107-Q](https://doi.org/10.1016/0047-6374(90)90107-Q).
29. Patikorn, C., Roubal, K., Veettil, S.K., Chandran, V., Pham, T., Lee, Y.Y., Giovannucci, E.L., Varady, K.A., and Chaiyakunapruk, N. (2021). Intermittent Fasting and Obesity-Related Health Outcomes: An Umbrella Review of Meta-analyses of Randomized Clinical Trials. *JAMA Netw. Open* 4, e2139558. <https://doi.org/10.1001/JAMANETWORKOPEN.2021.39558>.
30. Yin, W., Sun, L., Liang, Y., Luo, C., Feng, T., Zhang, Y., Zhang, W., and Yin, Y. (2023). Maternal intermittent fasting deteriorates offspring metabolism via suppression of hepatic mTORC1 signaling. *Faseb. J.* 37, e22831. <https://doi.org/10.1096/FJ.202201907R>.
31. Baylak, M.M., Sorochynska, O.M., Kuzniak, O.V., Gospodaryov, D.V., Demianchuk, O.I., Vasylyk, Y.V., Mosiichuk, N.M., Storey, K.B., Garaschuk, O., and Lushchak, V.I. (2021). Middle age as a turning point in mouse cerebral cortex energy and redox metabolism: Modulation by every-other-day fasting. *Exp. Gerontol.* 145, 111182. <https://doi.org/10.1016/J.EXGER.2020.111182>.
32. Lu, J., Lezi, E., Wang, W., Frontera, J., Zhu, H., Wang, W.T., Lee, P., Choi, I.Y., Brooks, W.M., Burns, J.M., et al. (2011). Alternate day fasting impacts the brain insulin-signaling pathway of young adult male C57BL/6 mice. *J. Neurochem.* 117, 154–163. <https://doi.org/10.1111/J.1471-4159.2011.07184.X>.
33. Subramanian, S., Khan, F., and Hirsch, I.B. (2024). New advances in type 1 diabetes. *BMJ* 384, e075681. <https://doi.org/10.1136/BMJ-2023-075681>.
34. Halban, P.A., Polonsky, K.S., Bowden, D.W., Hawkins, M.A., Ling, C., Mather, K.J., Powers, A.C., Rhodes, C.J., Sussel, L., and Weir, G.C. (2014).  $\beta$ -cell failure in type 2 diabetes: postulated mechanisms and prospects for prevention and treatment. *J. Clin. Endocrinol. Metab.* 99, 1983–1992. <https://doi.org/10.1210/JC.2014-1425>.
35. Kahn, S.E., and Porte, D. (1988). Islet dysfunction in non-insulin-dependent diabetes mellitus. *Am. J. Med.* 85, 4–8. [https://doi.org/10.1016/0002-9343\(88\)90392-0](https://doi.org/10.1016/0002-9343(88)90392-0).
36. Jeyarajan, S., Zhang, I.X., Arvan, P., Lentz, S.I., and Satin, L.S. (2023). Simultaneous Measurement of Changes in Mitochondrial and Endoplasmic Reticulum Free Calcium in Pancreatic Beta Cells. *Biosensors* 13, 382. <https://doi.org/10.3390/BIOS13030382>.
37. Liu, J.S.E., and Hebrok, M. (2017). All mixed up: defining roles for  $\beta$ -cell subtypes in mature islets. *Genes Dev.* 31, 228–240. <https://doi.org/10.1101/GAD.294389.116>.
38. Ardestani, A., Lupse, B., Kido, Y., Leibowitz, G., and Maedler, K. (2018). mTORC1 Signaling: A Double-Edged Sword in Diabetic  $\beta$  Cells. *Cell Metabol.* 27, 314–331. <https://doi.org/10.1016/j.cmet.2017.11.004>.
39. Longo, V.D., Di Tano, M., Mattson, M.P., and Guidi, N. (2021). Intermittent and periodic fasting, longevity and disease. *Nat. Aging* 1, 47–59. <https://doi.org/10.1038/S43587-020-00013-3>.
40. Munhoz, A.C., Vilas-Boas, E.A., Panveloski-Costa, A.C., Leite, J.S.M., Lucena, C.F., Riva, P., Emilio, H., and Carpinelli, A.R. (2020). Intermittent Fasting for Twelve Weeks Leads to Increases in Fat Mass and Hyperinsulinemia in Young Female Wistar Rats. *Nutrients* 12, 1029, Page 1029 12, 1029. <https://doi.org/10.3390/NU12041029>.

41. Habiby, M., Ezati, P., Soltanian, D., Rahehagh, R., and Hosseini, F. (2024). Comparison of three methods of intermittent fasting in high-fat-diet-induced obese mice. *Heliyon* 10, e25708. <https://doi.org/10.1016/J.HELLYON.2024.E25708>.
42. Al Rijjal, D., and Wheeler, M.B. (2022). A protocol for studying glucose homeostasis and islet function in mice. *STAR Protoc.* 3, 101171. <https://doi.org/10.1016/J.XPRO.2022.101171>.
43. Neuman, J.C., Truchan, N.A., Joseph, J.W., and Kimple, M.E. (2014). A method for mouse pancreatic islet isolation and intracellular cAMP determination. *J. Vis. Exp.* e50374. <https://doi.org/10.3791/50374>.
44. Zhu, Y.X., Zhou, Y.C., Zhang, Y., Sun, P., Chang, X.A., and Han, X. (2021). Protocol for in vivo and ex vivo assessments of glucose-stimulated insulin secretion in mouse islet  $\beta$  cells. *STAR Protoc.* 2, 100728. <https://doi.org/10.1016/J.XPRO.2021.100728>.
45. Fujimoto, K., Hanson, P.T., Tran, H., Ford, E.L., Han, Z., Johnson, J.D., Schmidt, R.E., Green, K.G., Wice, B.M., and Polonsky, K.S. (2009). Autophagy regulates pancreatic beta cell death in response to Pdx1 deficiency and nutrient deprivation. *J. Biol. Chem.* 284, 27664–27673. <https://doi.org/10.1074/JBC.M109.041616>.
46. Téllez, N., and Montanya, E. (2020). Determining Beta Cell Mass, Apoptosis, Proliferation, and Individual Beta Cell in Pancreatic Sections. *Methods Mol. Biol.* 2128, 313–337. [https://doi.org/10.1007/978-1-0716-0385-7\\_21](https://doi.org/10.1007/978-1-0716-0385-7_21).
47. McCarthy, D.J., Campbell, K.R., Lun, A.T.L., and Wills, Q.F. (2017). Scater: pre-processing, quality control, normalization and visualization of single-cell RNA-seq data in R. *Bioinformatics* 33, 1179–1186. <https://doi.org/10.1093/BIOINFORMATICS/BTW777>.
48. Stuart, T., Butler, A., Hoffman, P., Hafemeister, C., Papalexi, E., Mauck, W.M., Hao, Y., Stoeckius, M., Smibert, P., and Satija, R. (2019). Comprehensive Integration of Single-Cell Data. *Cell* 177, 1888–1902.e21. <https://doi.org/10.1016/J.CELL.2019.05.031>.
49. Butler, A., Hoffman, P., Smibert, P., Papalexi, E., and Satija, R. (2018). Integrating single-cell transcriptomic data across different conditions, technologies, and species. *Nat. Biotechnol.* 36, 411–420. <https://doi.org/10.1038/NBT.4096>.
50. Satija, R., Farrell, J.A., Gennert, D., Schier, A.F., and Regev, A. (2015). Spatial reconstruction of single-cell gene expression data. *Nat. Biotechnol.* 33, 495–502. <https://doi.org/10.1038/NBT.3192>.
51. Hafemeister, C., and Satija, R. (2019). Normalization and variance stabilization of single-cell RNA-seq data using regularized negative binomial regression. *Genome Biol.* 20, 296. <https://doi.org/10.1186/S13059-019-1874-1>.
52. Waltman, L., and van Eck, N.J. (2013). A smart local moving algorithm for large-scale modularity-based community detection. *Eur. Phys. J. B* 86, 471. <https://doi.org/10.1140/epjb/e2013-40829-0>.
53. Wolock, S.L., Lopez, R., and Klein, A.M. (2019). Scrublet: Computational Identification of Cell Doublets in Single-Cell Transcriptomic Data. *Cell Syst.* 8, 281–291.e9. <https://doi.org/10.1016/J.CELS.2018.11.005>.
54. Love, M.I., Huber, W., and Anders, S. (2014). Moderated estimation of fold change and dispersion for RNA-seq data with DESeq2. *Genome Biol.* 15, 550. <https://doi.org/10.1186/S13059-014-0550-8>.
55. Wu, T., Hu, E., Xu, S., Chen, M., Guo, P., Dai, Z., Feng, T., Zhou, L., Tang, W., Zhan, L., et al. (2021). clusterProfiler 4.0: A universal enrichment tool for interpreting omics data. *Innovation* 2, 100141, Cambridge (Mass.). <https://doi.org/10.1016/J.XINN.2021.100141>.
56. Guangchuang, Y., Erqiang, H., and Chun-Hui, G. (2023). Visualization of Functional Enrichment Result (Enrichplot). <https://doi.org/10.18129/B9.bioc.enrichplot>.
57. Tirosh, I., Izar, B., Prakadan, S.M., Wadsworth, M.H., Treacy, D., Trombetta, J.J., Rotem, A., Rodman, C., Lian, C., Murphy, G., et al. (2016). Dissecting the multicellular ecosystem of metastatic melanoma by single-cell RNA-seq. *Science* 352, 189–196. <https://doi.org/10.1126/SCIENCE.AAD0501>.
58. Wickham, H. (2016). ggplot2: Elegant Graphics for Data Analysis, Second Edition (Springer International Publishing). <https://doi.org/10.1007/978-3-319-24277-4>.
59. Gu, Z., Eils, R., and Schlesner, M. (2016). Complex heatmaps reveal patterns and correlations in multidimensional genomic data. *Bioinformatics* 32, 2847–2849. <https://doi.org/10.1093/BIOINFORMATICS/BTW313>.

## STAR★METHODS

### KEY RESOURCES TABLE

REAGENT or RESOURCE	SOURCE	IDENTIFIER
<b>Antibodies</b>		
Insulin (C27C9) Rabbit mAb	Cell Signaling	Cat# 3014. RRID: AB_2126503
Anti-Glucagon Mouse mAb	Sigma-Aldrich	Cat# G2654. RRID: AB_259852
4', 6-diamino-2-phenylindole - DAPI	Vector Laboratories	Cat#H1200. RRID: N/A
Mouse Anti-BrdU Monoclonal Antibody	Abcam	Cat#79737S. RRID: AB_2799938
MAFA (D2Z6N) Rabbit mAb #79737	Cell Signaling	Cat# ab98702. RRID: AB_10696531
GLUT2 Polyclonal Antibody	Bioss	Cat# bs-10379R. RRID: N/A
Human/Mouse NKX6.1 Antibody	R and D Systems	Cat# AF5857. RRID:AB_1857045
HLA-ABC Polyclonal Antibody	Thermo Fisher Scientific	Cat# PA5-115364, RRID:AB_2900000
Donkey Anti-rabbit Antibody, Alexa Fluor 594 Conjugated	Molecular Probes	Cat# A-21207. RRID: AB_141637
Donkey Anti-Goat IgG (H + L) Antibody, Alexa Fluor™ 555 Conjugated	Molecular Probes	Cat# A-21432, RRID:AB_141788
Goat anti-Rabbit IgG (H + L) Cross-Adsorbed Secondary Antibody, Alexa Fluor™ 750	Thermo Fisher Scientific	Cat# A-21039, RRID:AB_2535710
Donkey Anti-mouse Antibody, Alexa Fluor 488 Conjugated	Molecular Probes	Cat# A-21202. RRID: AB_141607
Goat polyclonal Secondary Antibody to Mouse IgG2b - (FITC)	Abcam	Cat# ab98702. RRID: AB_10696531
Goat anti-Mouse IgG H&L (Cy3) secondary antibody	Abcam	Cat# ab97035. RRID: AB_10680176
<b>Chemicals, peptides, and recombinant proteins</b>		
Roswell Park Memorial Institute (RPMI) Medium	Thermo Fisher	Cat# 1640/RRID: N/A
Krebs-Ringer Solution, HEPES-buffered	Thermo Fisher	Cat# J67795.K2 RRID: N/A
<b>Critical commercial assays</b>		
Ultra Sensitive Mouse Insulin ELISA Kit	Crystal Chem	Cat#90080. RRID: N/A
Histofix ® 4%	Roth	Cat# P087.3. RRID: N/A
<b>Deposited data</b>		
Raw and analyzed data – Figure 4G	This paper	GSE228267
Raw and analyzed data – Figure 4H	This paper	GSE164416
scRNA-seq – NCBI Gene Exp	This paper	GSE275356
<b>Experimental models: Organisms/strains</b>		
Male mice – Strain: C57BL/6N	Janvier Laboratory	RRID:MGI:2159965
<b>Software and algorithms</b>		
Prism (GraphPad) Version 9		<a href="https://www.graphpad.com/">https://www.graphpad.com/</a>
ImageJ		<a href="https://imagej.nih.gov/ij/">https://imagej.nih.gov/ij/</a>
The R Project for Statistical Computing v 4	CRAN	<a href="https://www.r-project.org/">https://www.r-project.org/</a>
Cell Ranger v2 & v3	10x Genomics	<a href="https://www.10xgenomics.com/support/software/cell-ranger/latest">https://www.10xgenomics.com/support/software/cell-ranger/latest</a>
Seurat v 3	CRAN	<a href="https://satijalab.org/seurat/articles/install_v5">https://satijalab.org/seurat/articles/install_v5</a>
DESeq2	Bioconductor	<a href="https://doi.org/10.18129/B9.bioc.DESeq2">https://doi.org/10.18129/B9.bioc.DESeq2</a>
ggplot2	CRAN	<a href="https://ggplot2.tidyverse.org/">https://ggplot2.tidyverse.org/</a>
ComplexHeatmap	Bioconductor	<a href="https://doi.org/10.18129/B9.bioc.ComplexHeatmap">https://doi.org/10.18129/B9.bioc.ComplexHeatmap</a>
<b>Other</b>		
ACCU-CHEK Performa	Roche	Cat#: 9055599. RRID: N/A

## EXPERIMENTAL MODEL AND STUDY PARTICIPANT DETAILS

### Mouse model

The study was approved by the government of Upper Bavaria, according to the protocol number: ROB-55.2-2532. Vet\_02-19-256, and performed by the Laboratory Animal Resources guidelines. Five-week-old male C57BL/6N mice were purchased from Janvier Laboratory. The colony was housed in groups of four, in a specific pathogen-free (SPF) facility in individually ventilated cages and a controlled environment (21°C–22°C, 30%–60% humidity) with free access to water and a standard rodent chow diet (18.9% protein, 5.5% fat, and 61.3% carbohydrate). All male mice were subdivided into three groups, to evaluate the effect of IF at different stages of life; the old group (eighteen months old); the middle-aged (eight months old), and the young (two months old).

## METHOD DETAILS

### Intermittent fasting

Old, middle-aged, and young mice were randomly grouped into *ad libitum* (AL) and intermittent fasting (IF) groups. In the IF group, the food was removed from 10 a.m. to the following day (24 h later), we employed the intermittent fasting protocol 1:2, which consists of 24 h of food starvation for 48 h of free access to a chow diet, an adaptation from protocols previously described and studied.<sup>39–41</sup> Mice in the AL group were handled similarly but with unrestricted chow diet access. For all groups, water was offered without restriction. Food intake was measured every three days, in the IF group we calculated the difference between the amount of food offered at the beginning of the food offer phase with the rest at the end of the phase. All groups, independently of age, were exposed to a period of 4–5 weeks (11 IF cycles) or 9–10 weeks (22 IF cycles) of the IF regimen and euthanized by cervical dislocation 48 h after the last IF cycle.

### Glucose tolerance tests (GTT) and insulin tolerance tests (ITT)

Mice were fasted for 6 h for GTT, and a hypertonic solution of glucose was administered intraperitoneally (2.5 g/kg). For ITT, we fasted the mice for 5 h (morning fasting) and insulin (0.8 units/kg) was injected intraperitoneally. Both tests measured blood glucose levels at 0, 15, 30, 60, 90, and 120 min after each injection. Blood glucose was measured using an Accu-Chek Performa glucose monitor (Roche Diagnostics, Castle Hill, Australia). Plasma insulin was measured using ELISA (Crystal Chem, Downers Grove, IL).<sup>42</sup>

### Islet isolation

Mice were sacrificed by cervical dislocation. The peritoneal cavity was exposed for clamping of the pancreatic main duct to the intestine and cannulation *in situ* via the common bile duct. Pancreata were inflated with a Collagenase P solution (2 U/ml in Hank's buffered salt solution (HBSS) supplemented with 1% BSA) and dissected, followed by an incubation in a 37°C water bath for 14 min. Islets were hand-picked four times in HBSS supplemented with 1% BSA, cultivated in Roswell Park Memorial Institute (RPMI) media containing 5.5 mmol/L glucose, 10% fetal bovine serum (FBS), and 1% penicillin and streptomycin solution, and incubated at 37°C and 5% CO<sub>2</sub>.<sup>43</sup>

### Insulin secretion and content assay

20 islets, with three replicates per animal, were washed twice in Krebs-Ringer HEPES buffer (containing 118.5 mM NaCl, 25 mmol/L NaHCO<sub>3</sub>, 1.19 mmol/L KH<sub>2</sub>PO<sub>4</sub>, 2.54 mmol/L CaCl<sub>2</sub>, 1.19 mM MgSO<sub>4</sub>, 4.74 mmol/L KCl, 10 mmol/L HEPES, and 0.1% BSA) supplemented with 1 mmol/L glucose. Islets were then starved in Krebs-Ringer HEPES Buffer containing 1 mmol/L glucose for 1 h at 37°C. Insulin secretion was stimulated at low glucose levels (LG - 2.8 mmol/L glucose), followed by high-glucose levels (HG - 16.7 mmol/L glucose), and potassium chloride (KCl - 20 mmol/L) for 30 min at 37°C. Islets were harvested in acid ethanol (1.5% HCl in 70% ethanol) to determine insulin content. Insulin levels were determined by ELISA following the manufacturer's instructions (Crystal Chem, Cat#90080, Downers Grove, IL). Insulin secretion and content were normalized to islet numbers.<sup>44</sup>

### Immunofluorescence

Dissected pancreas tissue was fixed in Formalin (Formalin 10% neutral buffered, HT501128, Sigma-Aldrich, Germany) for 24 h at Room Temperature and standardly processed for paraffin embedding (Tissue Tec VIP.6, Sakura Europe, Netherlands). Paraffinized pancreas was exhaustively cross sectioned into four parallel, equidistant slices per case. Maintaining their orientation, the tissue slices were vertically embedded in paraffin and cut into 3 µm slices. Following, short bouts of microwave exposure were used for antigen retrieval in a solution containing 1 mM EDTA, pH 8.0, for 15 min, followed by blocking in 1% BSA (Santa Cruz Biotechnology, sc-2323), 4% normal donkey serum (Abcam, AB166643) for 1 h at room temperature. Indirect immunofluorescence was performed using primary antibodies, rabbit anti-insulin (1:100; Cell Signaling Technology, Cat# 3014. RRID: AB\_2126503), and secondary antibodies, namely, Alexa Fluor 594 donkey anti-rabbit (1:500) and Alexa Fluor 488 donkey anti-mouse (1:500; Molecular Probes, Cat# A-21207. RRID: AB\_141637, and Molecular Probes, Cat# A-21202. RRID: AB\_141607, respectively). For maturation marker we used mouse anti-glucagon (1:500; Sigma-Aldrich, Cat# G2654. RRID: AB\_259852), rabbit anti-MAFA (1:100; Cell Signaling Technology, Cat# ab98702. RRID: AB\_10696531), rabbit anti-GLUT2 (1:100; BIOCSS, Cat# bs-10379R. RRID: N/A), goat anti-NKX6.1 (1:100; xxx), rabbit anti-HLA (1:100; R&D Systems, Cat# AF5857. RRID: AB\_1857045) as primary antibodies, and donkey anti-goat @555

(1:100; Molecular Probes, Cat# A-21432, RRID: AB\_141788) and goat anti-rabbit @750 (1:100; Thermo Fisher Scientific, Cat# A-21039, RRID: AB\_2535710) as secondary antibodies. Nuclei were stained with DAPI (Vector Laboratories, H1200). The stained tissue sections were scanned with an AxioScan 7 digital slide scanner (Zeiss, Jena, Germany) equipped with a 20× magnification objective. Quantification of respective target protein expression cells was performed on the entire tissue sections by using the image analysis software Visiopharm (Visiopharm, Hoersholm, Denmark). The islets were manually annotated, and the respective protein expression cells were classified automatically using the fluorescence intensity of each protein. The ratio of positive cells per total cells within the annotated islets was calculated for each target protein.<sup>45</sup>

### BrdU incorporation and detection

The procedure for BrdU labeling was previously described by Téllez, Noëlia, and Eduard Montanya.<sup>46</sup> Briefly, an analog of thymidine, BrdU (100 mg/kg body weight), was injected intraperitoneally twice a day for 5 days. For BrdU detection, the pancreas was collected and fixed in paraformaldehyde 4% before staining. The fixed pancreas slides were incubated with 0.5 M HCl at 37°C for 30 min for DNA denaturation. The slides were washed four times with PBS. Mouse anti-BrdU antibody (1:100; Abcam, Cat# ab8152, RRID: AB\_308713) was applied at 4°C for 16 h. A FIT-conjugated goat anti-mouse (1:10, Abcam, Cat# ab98702, RRID: AB\_10696531) or Cy3-conjugated sheep anti-mouse IgG (1:200, Abcam, Cat# ab97035, RRID: AB\_10680176) was used to reveal the BrdU incorporation.

### Single-cell RNA-Sequencing sample preparation and data Generation

For scRNA-seq, islets viability was measured and posteriorly dissociated using TrypLE Express (Gibco) for 12 to 20 min at 37°C. Cells were then washed with PBS containing 2% FCS, filtered through a 40 µm Flowmi Cell Strainer (Bel-Art), and diluted to a final concentration of ~1000 cells/µL in PBS containing 2% FCS. The cell suspension was immediately used for scRNA-seq library preparation with a target recovery of 10000 cells. Samples from young mice; MUC8408, MUC8409, MUC8410, MUC8411, MUC8412, MUC8413: Libraries were prepared using the Chromium Single Cell 3' Reagent Kits v2 (10x Genomics) according to the manufacturer's instructions. Libraries were pooled and sequenced on an Illumina HiSeq4000 with a target read depth of 50000 reads/cell. FASTQ files were aligned to the mm10 mouse genome with Ensembl release 94 annotations and pre-processed using the CellRanger software v2.1.1 (10x Genomics) for downstream analyses. Samples from middle-aged and old mice; MUC28169, MUC28170, MUC28171, MUC28172: Libraries were prepared using the Chromium Single Cell 3' Reagent Kits v3.1 (10x Genomics) according to the manufacturer's instructions. Libraries were pooled and sequenced on an Illumina NovaSeq6000 with a target read depth of 50000 reads/cell. FASTQ files were aligned to the GRCm38 mouse genome with Ensembl release 101 annotations and pre-processed using the CellRanger software v3.1.0 (10x Genomics) for downstream analyses.

### ScRNA-seq data processing, quality control, and analysis

Preprocessed count data were quality controlled with scatter 1.10.1,<sup>47</sup> imported into and analyzed by Seurat (v3).<sup>48–50</sup> Filtering of cells was based on more than 1500 but less than 8000 expression features in young mice and between 1500 and 5500 in the old group; for both mitochondrial fractions of reads <10%. For normalization and variance stabilization, we used the modeling framework sctransform,<sup>51</sup> following the Seurat v3 vignette “vignettes/sctransform\_vignette.Rmd”. Integration of individual samples has been performed using Pearson residuals as described in Seurat's SCTransform workflow. Dimensionality reduction plots are UMAP built with 30 PCs and confound removal was based on mitochondrial percentage after integration. Identification of statistical clusters was performed before duplex removal with Seurat's internal function “FindClusters” with the parameter resolution = 0.5. It is based on a shared nearest neighbor (SNN) modularity optimization method by Waltman L., and Van Eck N.<sup>52</sup> Cell identity classification and duplex removal: The canonical marker gene expression for the main endocrine cell types was extracted from the “RNA” slot and thresholded based on individual inspection of the data distributions (“Ppy” > 8.5, “Gcg” > 8, “Sst” > 4, “Ins1” > 8.7). Cells with high expression of exclusively one marker were used as pure profile cells in further analysis. Conserved marker genes have been identified for each of the four cell types from the pure profile cells and subsequently, centroids per cell type have been computed comprising all conserved marker genes from any of the pure profile cell types. In addition, artificial mixed-type centroids were computed for each pairwise and triple-cell combination. In the final step, transcriptomic profiles of all cells were individually correlated to all (pure and mixed) centroids and classified according to the highest correlation. Cells with the highest correlations to mixed centroids were finally removed as duplets. Quality control of classification was based on plausibility check in UMAPs, marker expression, and comparison to similar results obtained with the package “Scrublet”, as duplex removal.<sup>53</sup> Differential gene expression analysis was done using DESeq2 statistical models from the RNA assay with the function “FindMarkers” and min.pct = 0.3.<sup>54</sup> As there are no independent biological replicates, computation of statistical inference was based on individual beta-cells; N(Y-IF) = 3035; N(Y-AL) = 1568; N(M-IF) = 1891; N(M-AL) = 1503; N(O-IF) = 1182; N(O-AL) = 2013. Genes with  $p_{\text{val\_adj}} < 0.1$  &  $\text{abs}(\text{avg\_log2FC}) > 0.2$  were used for over-representation-based pathway analysis using clusterProfiler.<sup>55</sup> Visualizations were generated with dot plot and emap functions from the enrich plot package.<sup>56</sup> Computation of module scores was performed from the “SCT” Assay using Seurat's function “AddModuleScore” which utilizes the method by Tirosh.<sup>57</sup> Pairwise inference statistics within age groups were performed using non-parametric Wilcoxon tests with  $p$ -value adjustment for multiple testing by Holm. Visualization of single-cell data was performed with build Seurat functions, module score results and differential gene expression in volcano plots was done with ggplot2<sup>58</sup> and (log2FC) of candidate genes in heatmaps have been performed with the package “ComplexHeatmap”.<sup>59</sup>



### Gene Expression Omnibus data collection and analysis

We leveraged the Gene Expression Omnibus (GEO), a comprehensive public repository that amasses high-throughput sequencing and microarray datasets from global research entities, for our investigation. A systematic search was performed utilizing the keywords "Homo sapiens", "T1D", and "T2D" to pinpoint relevant expression datasets for our analysis. This search yielded two pertinent datasets, GSE164416 and GSE228267. Differential gene expression analysis between "healthy controls" and "patients" samples was executed using GEO2R, a user-friendly online utility that facilitates the comparison of datasets within a GEO series to identify differentially expressed genes under varying experimental paradigms. This analysis was carried out by employing the DESeq2 package, which utilized NCBI's computed raw count matrices as input. Statistical significance was ascertained through the adjusted P-value, applying the Benjamini-Hochberg method for controlling the false discovery rate. Criteria for statistical significance were set at a fold change threshold greater than 0.5 and an adjusted P-value of less than 0.05.

### Statistical analysis

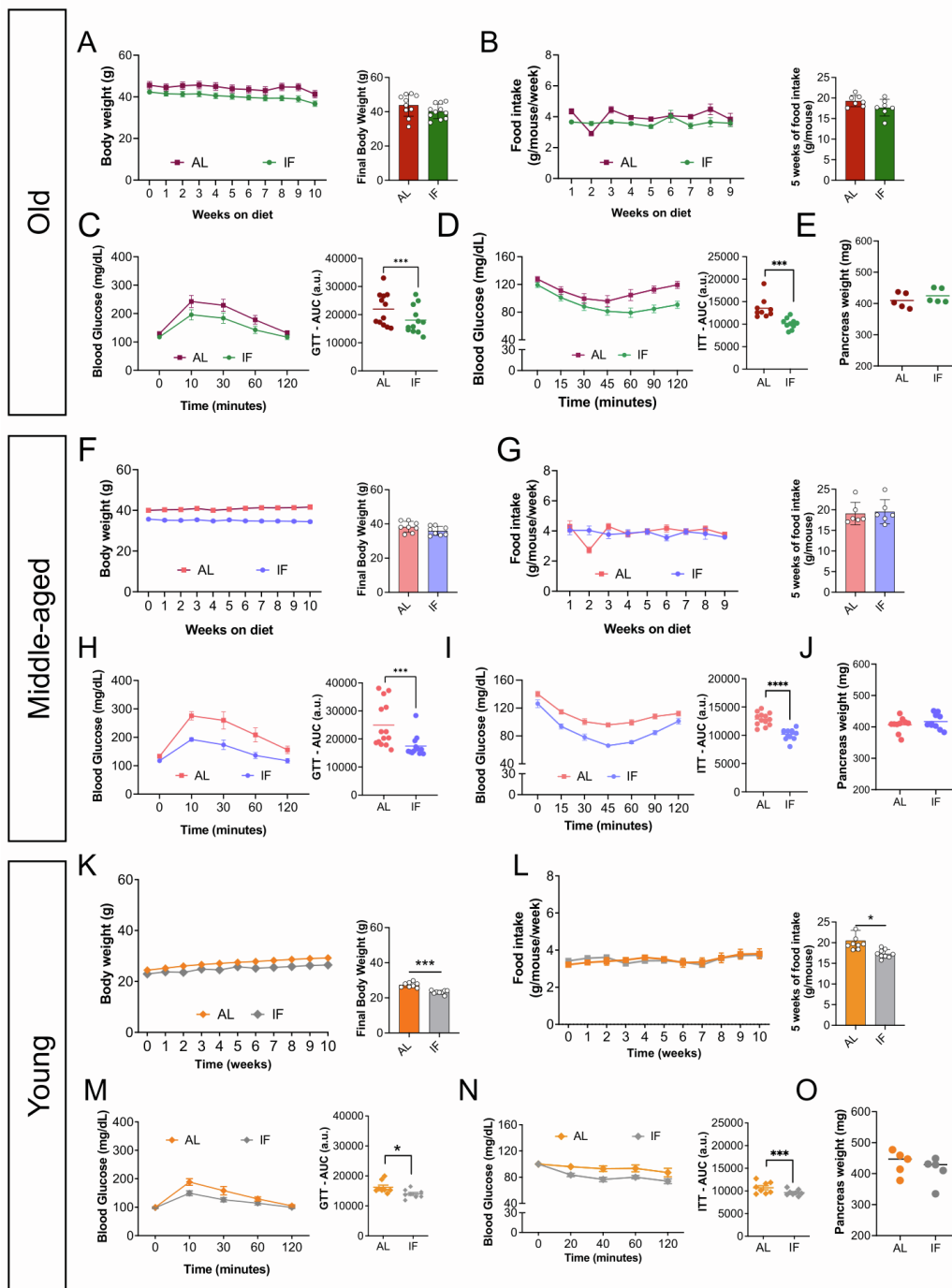
The data were expressed as mean  $\pm$  standard error of the mean (SEM) and D'Agostino and Pearson test was used to verify the normality of the samples, followed by the unpaired t test for the comparison between AL and IF groups in all aged groups. Comparisons involving three or more related groups were analyzed using the Kolmogorov-Smirnov test followed by a one-way ANOVA analysis of variance with Bonferroni multiple comparisons as post-test (i.e., [Figure 2](#)). Experiments involving histomorphometry measurements were performed in a blinded fashion, with randomly grouped mice. Sample size is described in each figure legend, and the minimum significance level established was  $p < 0.05$ . The results were analyzed through the statistical program GraphPad Prism 9.0 (San Diego, CA, USA).

**Supplemental information**

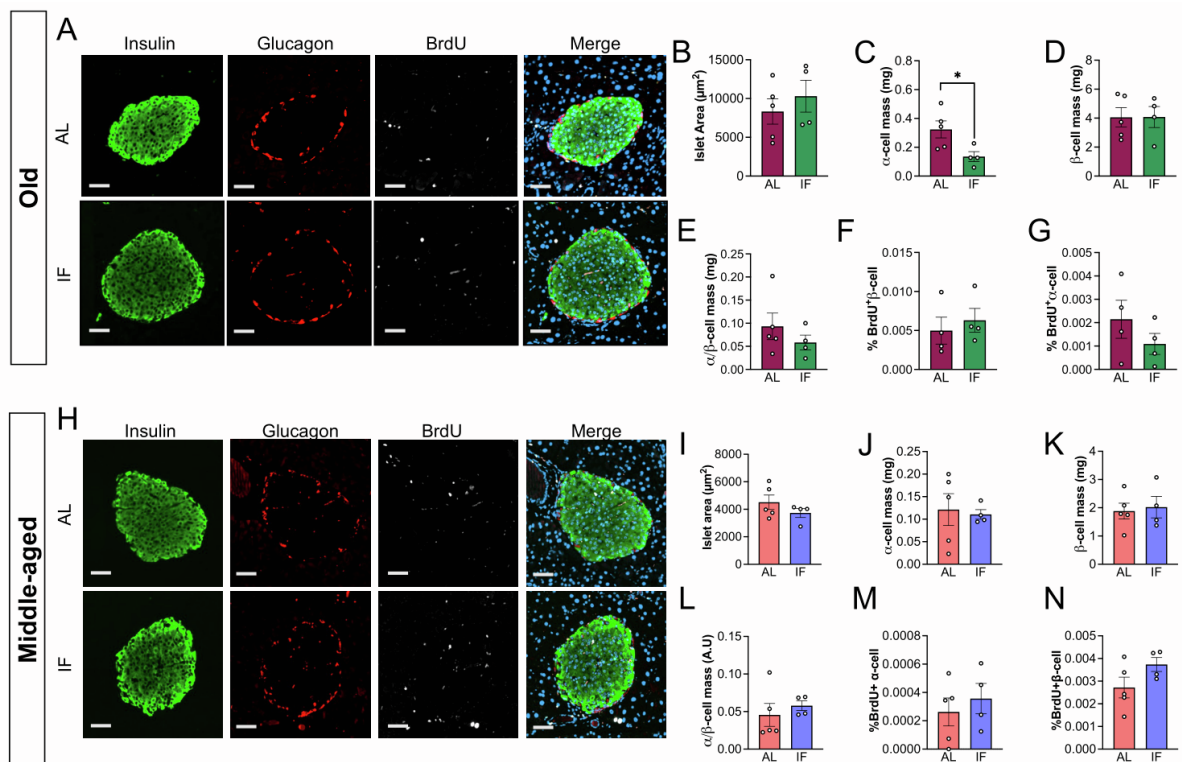
**Chronic intermittent fasting impairs  $\beta$  cell  
maturation and function in adolescent mice**

**Leonardo Matta, Peter Weber, Suheda Erener, Alina Walth-Hummel, Daniela Hass, Lea K. Bühler, Katarina Klepac, Julia Szendroedi, Joel Guerra, Maria Rohm, Michael Sterr, Heiko Lickert, Alexander Bartelt, and Stephan Herzig**

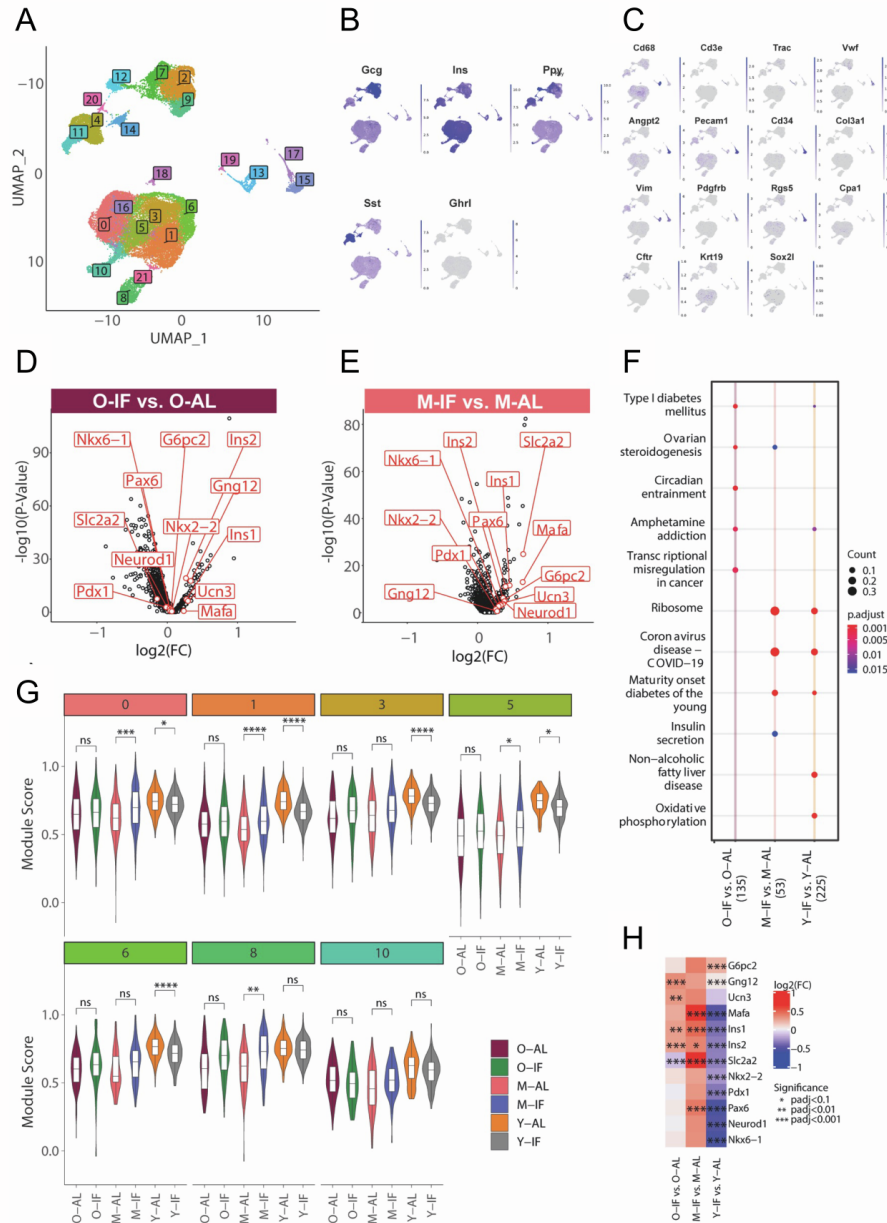
## Supplementary Material



**Supplementary figure 1. A short period of intermittent fasting intervention improves glucose homeostasis in all ages.** Body weight during and at the end of 5 weeks of dietary intervention (Old: a, Middle-aged: f, and young: k); Weekly and cumulative food intake (Old: b, Middle-aged: g, and young: l); Glucose tolerance test (2.5 mg/kg) after 5 weeks of IF intervention (Old: c, Middle-aged: h, and young: m); Insulin tolerance test (0.8 U/kg) after 5 weeks of IF intervention (Old: d, Middle-aged: i, and young: n); Pancreas Weight (Old: e, Middle-aged: j, and young: o). AL: Ad libitum; IF: Intermittent fasting; GTT: Glucose tolerance test; ITT: Insulin tolerance test and AUC: Area under curve. The data were expressed as the mean  $\pm$  standard error of the mean (Old: n = 9/group; middle-aged: n = 8/group; young mice: n = 8/group). Statistical differences, \*p < 0.05, \*\*\*p < 0.001.

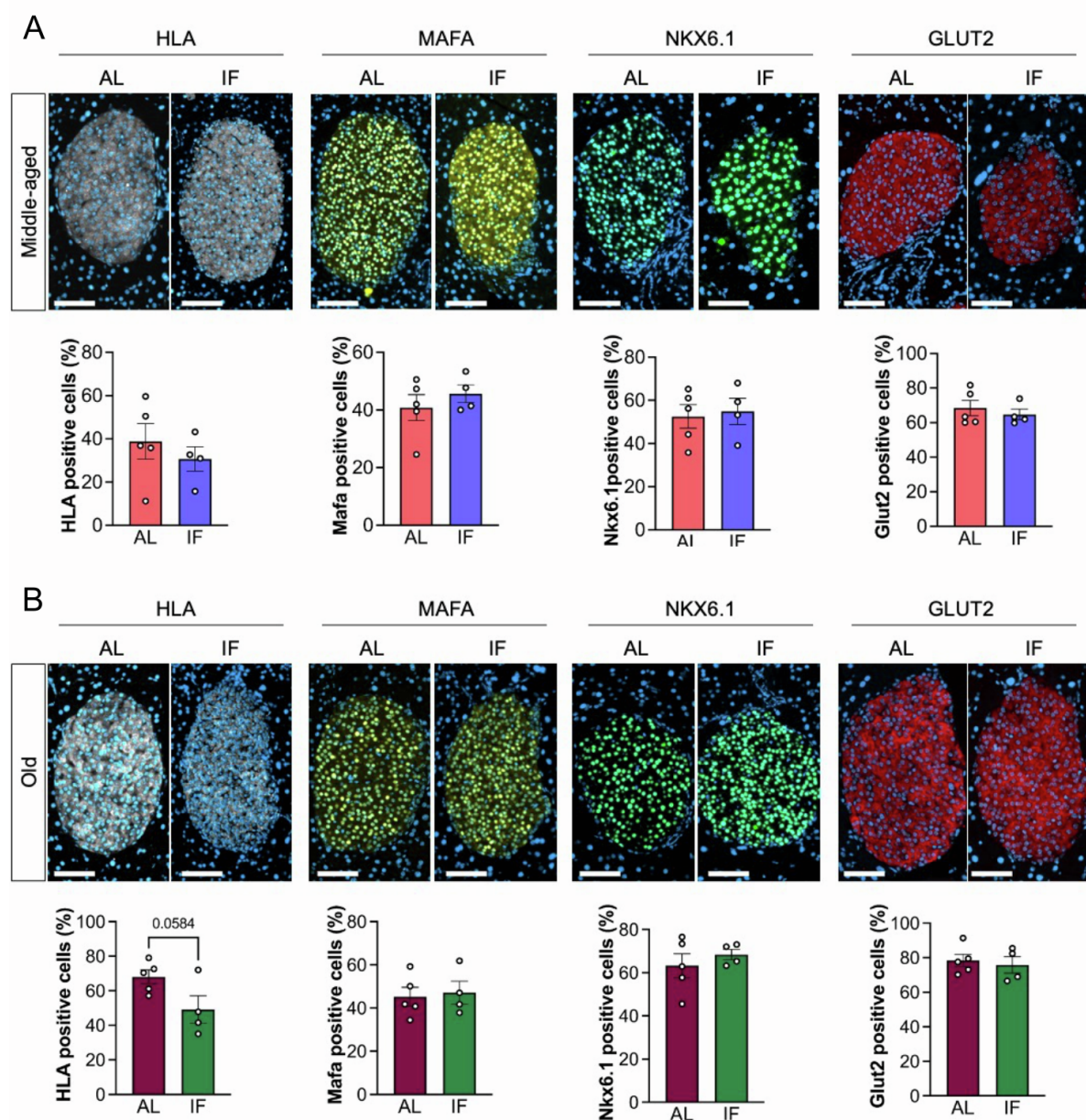


**Supplementary Figure 2. Long Intermittent fasting intervention does not affect islet morphology in old and middle-aged mice.** Immunofluorescence from pancreas of old- and middle-aged mice exposed to 10 weeks of intermittent fasting (a, h); Islet area  $\mu$ m<sup>2</sup> (b, i);  $\alpha$ -cell mass (c, j);  $\beta$ -cell mass (d, k);  $\alpha$ - and  $\beta$ - cell ratio (e, l); mass of  $\alpha$ - and  $\beta$ -cells positively stained for BrdU – proliferation (old: f and g; young m and n, respectively). Insulin positive cells: Green; Glucagon positive cells: Red; BrdU positive cells: White; and Nuclear staining (DAPI): Blue – Scale bar 100 $\mu$ m. AL: Ad libitum; IF: Intermittent fasting. The data is expressed as the mean  $\pm$  standard error of the mean (n=5 in the AL group and 3 in the IF group). Statistical differences, \*p<0.05, \*\*p <0.01.



**Supplementary Figure 3. Young mice exposed to long IF intervention present reduced transcriptomic activity scores for maturation and development also in subpopulations of  $\beta$ -cell.** UMAPs of scRNA-seq data indicating 22 statistical clusters (a), and expression of main markers for endocrine (b) as well as non-endocrine (c) cell types. Results of differential gene expression analysis upon IF vs. AL in old (d) and middle old (e) animals. Volcano plots show biological effect size ( $\log_2(\text{FC})$ ) on the x-axis and statistical significance ( $-\log_{10}(\text{P-value})$ ) on the y-axis. Comparison of over-representation analysis results of KEGG pathways in differentially expressed genes between all age groups (f). Comparison of module scores for beta cell maturation markers between IF and AL in all age groups for all beta cell clusters (g). Beta cell clusters with only a few cells have been excluded from this analysis (Clusters 16, 18 21). Heatmap of differential gene expression results ( $\log_2(\text{FC})$ ) of feeding intervention for all age groups (h). Feeding regimen-based experimental groups are intermittent fasting (IF) vs ad libitum (AL) in old (O-IF vs. O-AL), middle-aged (M-IF vs. M-AL), and young animals (Y-IF vs. Y-AL). Statistical significance is indicated with asterisks. \*  $\text{padj} < 0.05$ ; \*\*  $\text{padj} < 0.01$ ; \*\*\*  $\text{padj} < 0.001$ ; \*\*\*\*  $\text{padj} < 0.0001$  in (g) and (h).





**Supplementary Figure 4. Long Intermittent fasting intervention does not affect maturation-related protein expression in old and middle-aged mice.** Immunofluorescence from Pancreas from old- and middle-aged mice exposed to 10 weeks of intermittent fasting. HLA, Mafa, NKX6.1 and Glut 2 representative images and individual dot plot graphs from Middle-aged (a), and (b) old mice. Scale bar 50µm. AL: Ad libitum; IF: Intermittent fasting. The data is expressed as the mean  $\pm$  standard error of the mean.